Received: 7 April 2021 | Revised: 16 June 2021 | Accepted: 6 July 2021

DOI: 10.1111/jam.15217

Journal of Applied Microbiology

ORIGINAL ARTICLE

Distinct dynamics of *Vibrio parahaemolyticus* populations in two farming models

Qian Yang[1] | **Qingyao Wang**[2,3] | **Junmin Wu**[2,3] | **Yixiang Zhang**[4,5] | **Dawei Wei**[6] | **Baocheng Qu**[2,3] | **Ying Liu**[2,3] | **Songzhe Fu**[2,3]

[1]Center for Microbial Ecology and Technology (CMET), Ghent University, Ghent, Belgium

[2]College of Marine Science and Environment, Dalian Ocean University, Dalian, China

[3]Key Laboratory of Environment Controlled Aquaculture (KLECA), Ministry of Education, Dalian, China

[4]CAS Center for Excellence in Molecular Plant Sciences, Shanghai Institutes for Biological Sciences (SIBS), Chinese Academy of Sciences, Shanghai, China

[5]University of Chinese Academy of Sciences, Shanghai, China

[6]Institute of Microbiology, Chinese Academy of Sciences, Beijing, China

Correspondence
Songzhe Fu, College of Marine Science and Environment, Dalian Ocean University, Dalian, China; Key Laboratory of Environment Controlled Aquaculture (KLECA), Ministry of Education, 116023 Dalian, China.
Email: fusongzhe@dlou.edu.cn

Funding information
National Natural Science Foundation of China, Grant/Award Number: 81903372; Youth Fund of Liaoning Provincial Department of Education, Grant/Award Number: QL202005; Key R&D Program of Guangdong Province, Grant/Award Number: 2019B020215001 and GML2019ZD0402; Special Research Fund of Ghent University

Abstract

Aims: Despite the recent prosperity of shrimp cultivation in China, very little is known about how different shrimp farming models influence the dynamics of *Vibrio parahaemolyticus* populations and the antibiotic resistance of this bacterium.

Methods and Results: To this end, we conducted continuous surveillance of *V. parahaemolyticus* on four farms over 3 years: two traditional shrimp farms with daily water exchange and two farms operated in the recirculating aquaculture systems (RAS). No antibiotics were used in these farms to exclude the potential impacts of antibiotics on the emergence of antibacterial resistance. Multilocus sequence typing was utilized to characterize the dynamics of *V. parahaemolyticus* populations. Whole-genome sequencing (WGS) was conducted to determine the representative sequence types (STs) at each farm. Results revealed that the population structure of *V. parahaemolyticus* remained stable over time in both RAS farms, with only nine and four STs observed at each. In contrast, annual replacement of *V. parahaemolyticus* populations was observed in traditional farms with 26 and 28 STs identified in rearing water. WGS of 50 isolates divided them into five clusters, of which ST917a isolates harboured a genomic island that disrupted the gene *recA*. Pair-wised genomic comparison of isolates from the same STs showed that they were genetically related but belonged to different clones associated with geographical distribution.

Conclusions: These results suggested that RAS presented a specific ecological niche by minimizing the water exchanges with the external environment. In contrast, traditional farming might pose a food safety issue by introducing new *V. parahaemolyticus* populations with antibiotic resistance genes.

Significance and Impact of the Study: Our results expose the potential food safety issue associated with conventional agriculture and should encourage the development of preventive strategies to reduce the emergence of resistant *V. parahaemolyticus* populations.

KEYWORDS

MLST, re-circulating aquaculture system, traditional farming, *Vibrio parahaemolyticus*, whole-genome sequencing

Qian Yang and Qingyao Wang contributed equally to this paper.

INTRODUCTION

Vibrio parahaemolyticus is a halophilic foodborne bacterium widespread in aquacultural and oceanic environments (Yang et al., 2019). It is currently the primary cause of seafood-borne acute gastroenteritis in humans and has severely impacted shrimp aquaculture globally, resulting in significant economic losses (FAO, 2013). *V. parahaemolyticus* is frequently isolated from diseased shrimp and the sediments of devastated shrimp farms (Fu et al., 2017; Yang et al., 2019). Various types of antibiotics have been utilized to control the progression of the disease, resulting in the emergence of multi-drug resistant (MDR) *V. parahaemolyticus* (Xie et al., 2020). *V. parahaemolyticus* strains harbouring colistin resistance gene *mcr-1* were also recently identified, presenting a significant threat to public health (Lei et al., 2019). The heavy use of antibiotics also triggered the frequent horizontal gene transfer (HGT) of resistant and virulent genomic islands amongst the various genotypes of *V. parahaemolyticus* in shrimp ponds (Fu et al., 2021a). To further distinguish the genotype of *V. parahaemolyticus*, multilocus sequence typing (MLST) based on sequence polymorphisms of seven housekeeping genes has been established to prospectively identify the genotypes of *V. parahaemolyticus* (González-Escalona et al., 2008).

Currently, there are two major farming models for shrimp production in China, traditional farming and recirculating aquaculture farms. Traditional pond farming (TF) requires 10–20% daily water exchange to maintain high water quality and often results in the introduction of external pathogens (Birkett et al., 2020). Owing to the relatively low cost for infrastructure, low requirement for water management and plentiful water supply, it is currently the most extensive farming model for shrimp cultivation in China. However, this model significantly impacts the environment, degrading coastal wetlands, increasing pollution and inducing the extinction of indigenous species (Burbridge & Hellin, 2000). On the other hand, recirculating aquaculture systems (RAS) use significantly less water, with only 0.3–1% daily water exchange.

RAS is another model in modern aquaculture with 0.3–1% daily water exchange. Due to lower water requirements and lower discharge of wastewater, there are several advantages in using RAS over traditional farming systems in controlling pollution and improving biosecurity, which could efficiently limit the entrance of external pathogens (Attramadal et al., 2014). However, this model requires high cost of investments for infrastructure, sophisticated management of water treatment facilities and highly skilled workers, which hinders the widespread application in China.

To date, very little is known about the long-term dynamics of *V. parahaemolyticus* populations in different farming models and their impacts on the food safety of aquatic animals. Intensive aquacultural activities in traditional farms might also provide a suitable niche for HGT between *Vibrio* spp. and other bacteria (Fu et al., 2021b). However, there is no long-term surveillance on *V. parahaemolyticus* populations in these two shrimp aquaculture models.

In this study, we conducted pathogen surveillance in two RAS farms and two traditional farms in Liaoning and Zhanjiang, respectively, whilst no pathogenic genes have been observed (Figure S1). MLST was first employed to describe the dynamics of *V. parahaemolyticus* populations under both aquaculture models; then, we sequenced isolates from the same sequence types (STs) isolated in different years or at different sites to confirm their epidemiological relatedness. These results provide a broader understanding of the dynamics of *V. parahaemolyticus* populations in different shrimp farming models, facilitating the development of preventive strategies for reducing the future emergence of resistant populations.

MATERIAL AND METHODS

Sampling sites

Two typical shrimp farming regions were selected from Liaoning and Guangdong province in China, respectively (Figure S1a). Liaoning province has a long history for shrimp farming in North China, which has the highest production of Chinese shrimp (*Penaeus chinensis*) (Xie & Yu, 2007). One TF farm in Yingkou and one RAS farm in Dalian were selected for continuous pathogen surveillance with a 50-km distance (Figure 1b). Both farms included six shrimp ponds with 1000-L rearing water in each pond. To exclude the impacts of antibiotic treatment on the evolution, both farms were operated without antibiotic usage. In the TF farm, water exchange was maintained at 15–20% relative to the volume of shrimp pond daily to ensure water quality, whereas for the RAS farm, which consisted of ponds and wastewater treatment unit, a small amount of underground seawater (relative to 0.5% volume of shrimp pond) was transferred into the shrimp pond daily to compensate for water evaporation. During the cultivation, the water temperatures were maintained at 28 for both farms.

Another sampling site is located in the southernmost regions of China called Zhanjiang, which is China's top region for white shrimp (*Penaeus vannamei*) cultivation (Figure S1c). One TF farm with a daily water exchange of 15% and one RAS farm with 0.3% daily water exchange were selected within a 5-km distance. Both farms included four shrimp ponds with 1000-L rearing water in each pond. For all sampled farms, microbiological analysis was conducted for post-larval shrimp before farming to guarantee no pathogen would be introduced by shrimp as described by Zorrilla et al., (2003).

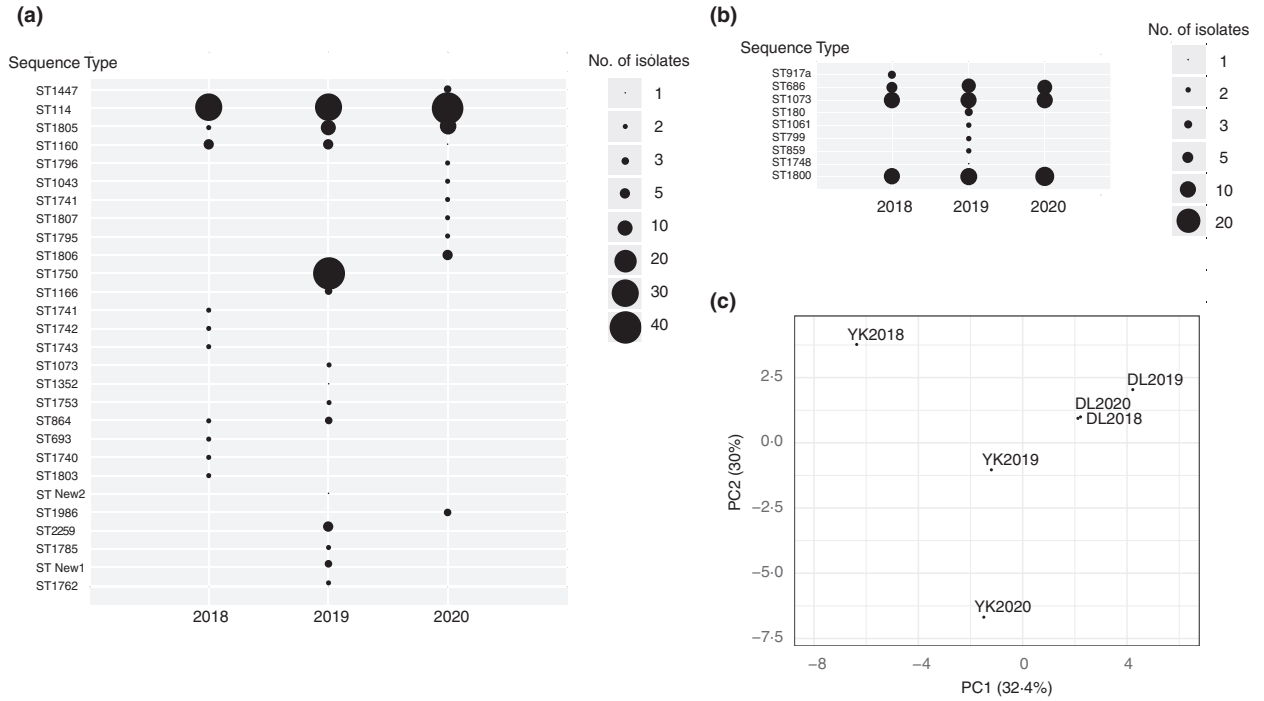

FIGURE 1 Dynamics of *V. parahaemolyticus* populations in two farms of Liaodong Peninsula. (a) Dynamics of *V. parahaemolyticus* sequence types in Yingkou traditional farm from 2018 to 2020; (b) Dynamics of *V. parahaemolyticus* sequence types in Dalian RAS farm from 2018 to 2020; (c) Principal coordinate analysis (PCoA) based on Bray–Curtis dissimilarity of *V. parahaemolyticus* community composition of different samples collected from Yingkou and Dalian based on the composition of STs. DL2018, DL2019 and DL2020 denote Dalian samples collected in 2018, 2019 and 2020, respectively; YK2018, YK2019, YK2020 denote samples collected from Yingkou in 2018, 2019 and 2020, respectively. RAS, recirculating aquaculture systems; ST, sequence types

Sample collection in four shrimp farms

In November 2016–2018, triplicate water samples were simultaneously collected from both farms in Zhanjiang. From 2018 to 2020, samples of rearing water were also simultaneously collected from two farms from Dalian and Yingkou. Triplicate water samples were also collected in August from both farms. Rearing water samples (1000 mL) were collected at 0.5-m depths of shrimp pond using sterile Niskin bottles and transferred to sterile plastic containers. For TF farms, three water samples were, respectively, collected from three shrimp ponds with 50-m distance. Three sampling ponds were selected for RAS farms at the plants' entrance, central, and exit sites.

Bacteria isolation, identification, and MLST

For each sample, 1000 mL of water was filtered through 0.45-μm pore-size polycarbonate membranes (Millipore Corporation) using a vacuum pump. The filters were immediately placed on thiosulfate-citrate-bile salt-sucrose agar and incubated at 30°C for 24 h. After incubation, green colonies were picked as presumptive *V. parahaemolyticus* isolates and were further verified by polymerase chain reaction (PCR) to detect the presence of *V. parahaemolyticus*-specific *tlh* gene (Niu et al., 2018).

Conventional MLST was performed on a subset of *V. parahaemolyticus* isolates, as previously described (González-Escalona et al., 2008). Sequencing was performed at the nucleotide sequences, and deduced protein sequences were analysed with EditSeq and MegAlign software (DNASTAR). The STs that found in multiple years or various locations were selected for WGS.

Antibiotics susceptibility test

Antimicrobial susceptibility test for 12 antibiotics including ampicillin (10 μg), amikacin (30 μg), tetracycline (30 μg), chloramphenicol (30 μg), ciprofloxacin (5 μg), enrofloxacin (5 μg), florfenicol (30 μg), oxytetracycline (30 μg), rifampicin (5 μg), sulfamethoxazole (300 μg), trimethoprim (5 μg) and tetracycline (30 μg) was performed using broth microdilution assay according to the protocol of Thermo Scientific Sensititre Custom Plate (Thermo Fisher Scientific). The results were classified into susceptible, intermediate or resistant phenotype based on the protocol of the Clinical and Laboratory Standards Institute (CLSI, 2006).

WGS, *de novo* assembly and annotation

Total bacterial DNA was extracted from an overnight culture with the Wizard Genomic DNA Kit (Promega). High-throughput genome sequencing was carried out on Illumina platforms or Pacbio RSII platform at Beijing Novogene Bioinformatics Technology Co., Ltd. The FASTQ reads were quality trimmed with Trimmomatic (v0.36) (Bolger et al., 2014), and bases with a PHRED score of <30 were removed from the trailing end. The draft genome was assembled *de novo* with SPAdes version 3.0 (Bankevich et al., 2012). Antimicrobial resistance genes were identified with ResFinder (Zankari et al., 2012). Rapid Annotation using Subsystem Technology (RAST) was used to annotate the sequences of each genome determined with next-generation sequencing (Aziz et al., 2008).

Identification of single nucleotide polymorphisms (SNPs) and phylogenetic analyses

The core genome of *V. parahaemolyticus* defined by González-Escalona et al., (2017) was used as the reference genomes to call the SNPs for *V. parahaemolyticus*. SNP calling was performed with a previously developed pipeline to guarantee that only genuine SNPs were included in the analysis (Chan et al., 2016). Raw SNP calls were filtered for quality scores of ≥20, with a cutoff of 20 reads covering the SNP site and ≥70% of the reads supporting the SNP. We filtered out the SNPs with low sequence quality (quality score <20 or was covered by <10 reads). SNPs in the recombination regions were removed by Clonalframe ML (Didelot & Wilson, 2015).

Randomized Axelerated Maximum Likelihood (RAxML) version 7.8.6 was used with the generalized time-reversible model and a Gamma distribution to model site-specific rate variation (the GTR+⌈ substitution model; GTRGAMMA in RAxML) (Stamatakis, 2006). Support for the ML phylogeny was assessed by 100 bootstrap pseudoanalyses of the alignment data, and the final tree was visualized in FigTree version 1.4.2 (http://tree.bio.ed.ac.uk/software/figtree/). Artemis comparison tool was used to compare the genomes (Carver et al., 2012). BLASTn was used to compare the sequences with the nucleotide databases in NCBI (Altschul et al., 1990).

Statistical analyses

Averages and standard deviations were computed using the base function in R package version 3.4.1 (R Development Core Team, 2014). Principal coordinates analysis (PCoA) based on Bray–Curtis distance were made on R 3.4.1 in the vegan package to compare the dissimilarity of bacterial composition (Oksanen et al., 2019).

RESULTS

Dynamics of *V. parahaemolyticus* populations in TF and RAS farms in Liaoning

In Yingkou TF farm, we obtained 63, 100 and 68 V. *parahaemolyticus* isolates in 2018, 2019 and 2020, respectively, which were divided into 10, 12 and 11 types of STs (Figure 1a). The Good's coverage value ranged from 87.5% to 88.89%, which were adequate for local communities (Table 1), whereas the Shannon index values ranged from 1.37 to 2.16. Furthermore, distinct STs of *V. parahaemolyticus* communities prevailed in Yingkou in different years (Figure 1a). In 2018, shrimp pond mainly consisted of ST114 (49.2%), ST1160 (7.9%) and ST1805 (7.9%), whereas in 2019, ST114 was still the predominant ST (27.5%). However, the relative abundance of ST1750 and ST1805 accounted for 26.7% and 7.5%, respectively. In 2020, ST114 (60.3%) and ST1805 (16.2%) became the predominant STs.

In addition, in Dalian RAS farm, 28, 40 and 35 V. *parahaemolyticus* isolates were obtained in 2018, 2019 and 2020, respectively, which were subtyped into 4, 8 and 3 STs, respectively (Figure 1b). The Good's coverage value of each sample ranged from 87.5% to 100%, indicating a significant contribution of *V. parahaemolyticus* population (Table 1). The Shannon index values ranged from 1.08 to 1.78, whereas the Simpson index ranged from 0.65 to 0.80.

ST686, ST1073 and ST1800 were the most abundant STs in 2018, with an average relative abundance of 35.7%. In 2019, ST686 (25%), ST1073 (25%) and ST1800 (25%) were the predominant STs, whereas in 2020, ST686 (28.6%), ST1073 (28.6%), and ST1800 (42.9%) became the predominant STs (Figure 1b). Taken together, ST686, ST1073 and ST1800 accounted for 82.5% of *V. parahaemolyticus* isolates in the RAS farm, indicating that shrimp ponds were stably dominated by these STs.

We also compared the effects of two aquaculture models on the community composition of *V. parahaemolyticus* by PCoA (Figure 1c). *V. parahaemolyticus* community composition in Yingkou TF farm displayed tempo heterogeneity, as clustering occurred according to sampling time (analysis of similarities [ANOSIM], $p < 0.001$), but no significant tempo shifts were observed in Dalian RAS farm. In addition, significant spatial heterogeneity was observed in the two farms (ANOSIM, $p < 0.001$).

Dynamics of *V. parahaemolyticus* populations in traditional and RAS farms in the Zhanjiang region

In a traditional farm of Zhanjiang, we obtained 41, 35 and 47 V. *parahaemolyticus* isolates in 2016, 2017 and 2018, respectively, which were divided into 16, 7 and 11 STs (Figure 2a). The Good's coverage value ranged from 83.33% to

TABLE 1 Diversity indices and richness index of each sampling site[a]

Sample ID	No. of STs	No. of clones	No. of singleton ST	Good's coverage (%)	Simpson diversity	Shannon diversity
YK2018	10	56	0	100.00	0.73	1.86
YK2019	14	100	2	87.50	0.84	2.16
YK2020	9	68	1	88.89	0.60	1.37
DL2018	4	28	0	100.00	0.70	1.28
DL2019	8	40	1	87.50	0.80	1.78
DL2020	3	35	0	100.00	0.65	1.08
ZJ2016	16	41	1	93.75	0.93	3.88
ZJ2017	8	35	0	100.00	0.85	2.57
ZJ2018	12	47	2	83.33	0.78	2.77
RAS2016	3	15	1	66.67	0.47	1.05
RAS2017	3	16	0	100.00	0.65	1.55
RAS2018	3	19	0	100.00	0.63	1.51

[a]Shannon index ($H = -\sum Pi*\ln Pi$), Simpson index ($D = 1 - \sum Pi^2$); $C = 1 - n1/N$, n1 is the number of singleton, whilst N is the total number of ST. YK2018, YK2019 and YK2020 denote samples collected from Yingkou in 2018, 2019 and 2020, respectively; DL2018, DL2019, and DL2020 denote Dalian samples collected in 2018, 2019 and 2020, respectively. RAS2016, RAS2017 and RAS2018 denote samples collected from RAS farm in Zhanjiang in 2016, 2017 and 2018, respectively; ZJ2016, ZJ2017 and ZJ2018 denote samples collected from traditional farm in Zhanjiang in 2016, 2017 and 2018, respectively. RAS, recirculating aquaculture systems; ST, sequence type.

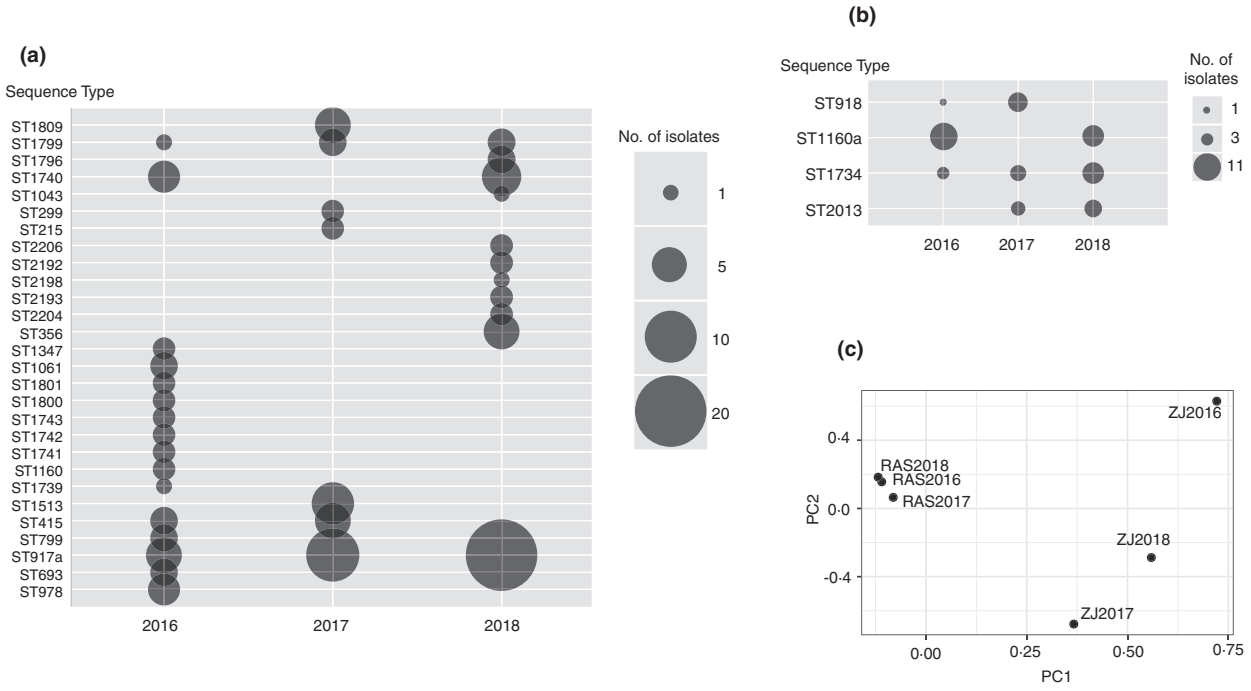

FIGURE 2 Dynamics of *V. parahaemolyticus* populations in two farms of Leizhou Peninsula. (a) Dynamics of *V. parahaemolyticus* sequence types in Maoming traditional farm from 2016 to 2019; (b) Dynamics of *V. parahaemolyticus* sequence types in Maoming RAS farm from 2016 to 2019; (c) Principal coordinate analysis (PCoA) based on Bray–Curtis dissimilarity of *V. parahaemolyticus* community composition of different samples collected from traditional farm and RAS farm in Zhanjiang based on the composition of STs. RAS2016, RAS2017 and RAS2018 denote samples collected from RAS farm in Zhanjiang in 2016, 2017 and 2018, respectively; ZJ2016, ZJ2017, ZJ2018 denote samples collected from traditional farm in Zhanjiang in 2016, 2017 and 2018, respectively. RAS, recirculating aquaculture systems; ST, sequence types

93.75%, which were appropriate numbers for local communities (Table 1). Distinct *V. parahaemolyticus* STs were found in different years in this traditional farm (Figure 2a). From 2016 to 2018, shrimp pond mainly consisted of ST917a (28.7%), ST1740 (7.6%) and ST415 (7.2%). However, other STs such as ST1799, ST1513 and ST1809 also contributed with over 5%.

The Shannon index values ranged from 2.57 to 3.88, whereas the Simpson index ranged from 0.78 and 0.93 (Table 1).

Furthermore, in the RAS farm, we obtained 15, 16 and 19 V. *parahaemolyticus* isolates in 2016, 2017 and 2018, respectively. Only four types of STs were found during the study period, including ST918, ST1734, ST2013 and a variant of ST1160 (namely ST1160a), indicating that shrimp ponds in this RAS farm were stably dominated by these STs. *V. parahaemolyticus* isolates were typed into three STs each year (Figure 2b). The Good's coverage value of each sample ranged from 66.7% to 100% (Table 1).

In addition, we compared the effects of two aquaculture models on the dynamics of *V. parahaemolyticus* populations by PCoA (Figure 2c). The community composition of *V. parahaemolyticus* in the traditional farm displayed significant tempo heterogeneity (ANOSIM, $p < 0.001$), but no significant tempo shifts were observed in the RAS farm.

Phylogenetic analysis of *V. parahaemolyticus* isolates in four farms

To further understand the genetic relationships of *V. parahaemolyticus* isolates within the same STs, we selected isolates that were from the same STs for sequencing, which were isolated in different years or at different sites. By using this criterion, 50 isolates were selected from 18 STs from four seafood farms, which were subjected to WGS. To determine the phylogenetic relationships amongst shrimp pond isolates, a core genome SNPs-based genomic tree was generated using the maximum likelihood method (Figure 3a). Phylogenetic analysis divided them into six clusters. All of the serial *V. parahaemolyticus* isolates from the same ST were grouped together.

To obtain the highest resolution relationships of isolates within an ST, we further calculated pair-wise SNPs differences for ST1740, ST864, ST114, ST1799, ST1160, ST1073 and ST917a from two traditional farms, separately. These STs contained multiple geographically and temporally variable isolates. Isolates from other regions in the public dataset were also included. We described the results by grouping STs to observe genomic variations. ST114 isolates from five locations were geographically distinct (Figure 3b), of which Yingkou isolates were clustered with Dalian isolates identified in our previous study (Fu et al., 2021b). Relative to other Yingkou isolates, VP14-2020 had only one SNP. Similarly, genomic analysis of ST864 isolates from three sites revealed that they were divided into three clusters, of which Yingkou

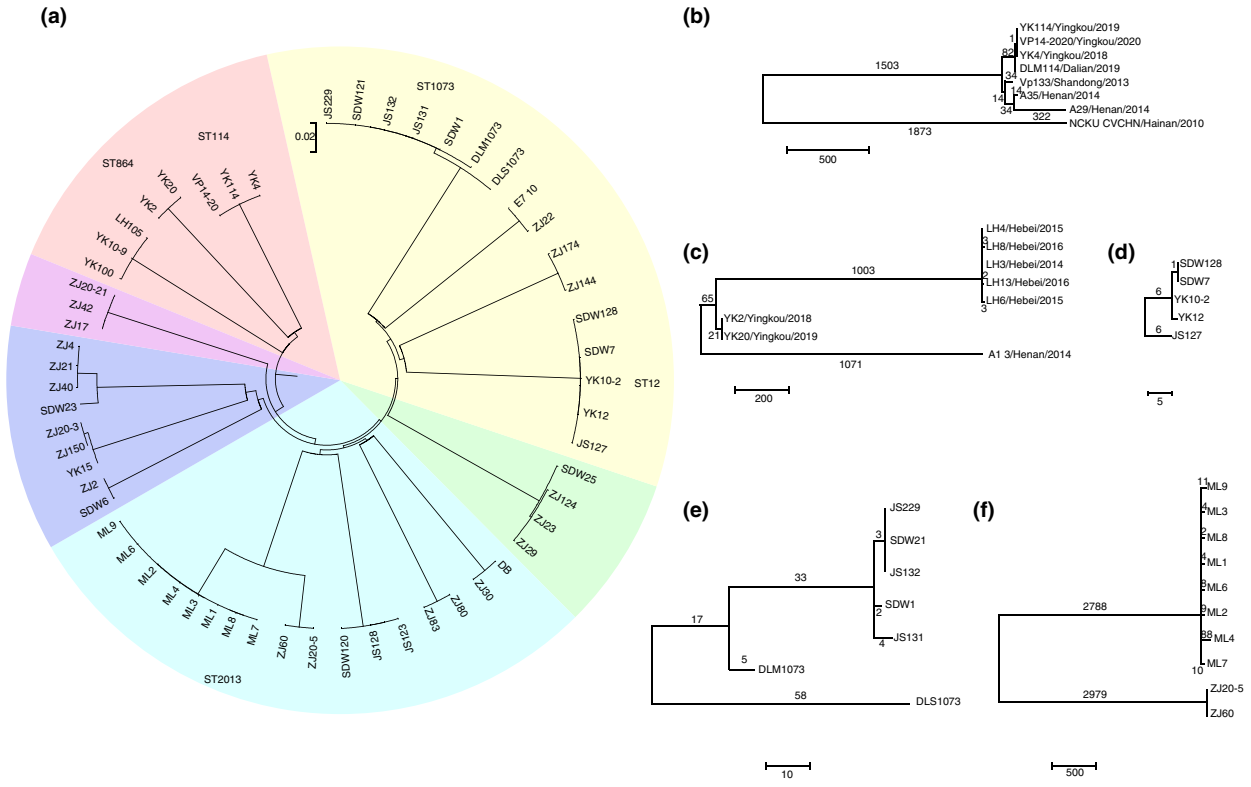

FIGURE 3 Phylogeny analysis of the 50 V. *parahaemolyticus* genomes from four farms. Maximum-likelihood (ML) method was used to infer the genomic relationship of *V. parahaemolyticus* genomes (a). The scale bar denotes substitutions per variable site. Phylogenetic analysis of ST114 (b), ST864 (c), ST12 (d), ST1073 (e) and ST2013 (f) isolates. Maximum parsimony method was used to infer the phylogenetic relationship of the isolates within the same STs. The number of SNPs is indicated above the branch. The scale bar indicates the number of SNPs. SNPs, single nucleotide polymorphisms

isolates were grouped with 1024 SNP differences to Hebei isolates. Moreover, two ST1740 isolates found in Zhanjiang had 114 SNP difference relative to ST1740 isolate YK15 obtained from Yingkou (Figure 3a).

For the isolates with one locus difference in the MLST scheme, the genomic analysis revealed that three ST1799 isolates differed by 14 SNPs and had 514 SNP differences relative to ST180 isolate SDW23. The ST1160 isolate had 611 SNP differences, with two isolates belonging to ST1160a. ST917a isolates were found in Dalian and Zhanjiang but had 423 SNP differences (Figure 3c).

For RAS farms, only three SNPs were identified in 2020 ST686 strains, compared with ST686 isolates in 2018 and 2019. Five ST12 isolates have 14 SNP difference (Figure 3d), whereas SNPs were not present in ST918 and ST1734 isolates. Similarly, ST1073 isolates had a maximum of only 10 SNP differences within the Dalian shrimp farms in 3 years. Still, they had more than 50 SNP differences with the two isolates from other shellfish farms in Dalian (Figure 3e). Genomic analysis of ST2013 isolates divided Zhanjiang and Malaysia isolates into two clusters, differing by 5767 SNPs, suggesting an early genomic divergence between two sites (Figure 3f).

Antibiotic resistance patterns of isolates in two farming models

Antimicrobial susceptibility testing was performed on 115 representative isolates selected from each STs. Results revealed antibiotic resistance only to ampicillin in most RAS isolates (Table S1). Only two ST1160a and two ST180 isolates showed resistance to tetracycline (Table S1). In contrast, 50% and 33.7% of isolates from traditional farms evidenced resistance to more than two types of antibiotics in Yingkou and Zhanjiang, respectively (Figure 4). Notably, 6.9% Yingkou isolates and 7.3% Zhanjiang isolates harboured resistance to more than six types of antibiotics. Genomic analysis of sequenced isolates further identified the type of antibiotic resistance genes. For instance, ST1740 isolates harboured three resistant genes including $bla_{\text{CARB-20}}$, *tet(59)* and *sul2*, whereas ST1160 harboured $bla_{\text{CARB-33}}$, *tet(59)* and *sul2* (Table S1).

Genomic analysis of the genomic island around the *recA* sites in ST917a isolates and public genomes

ST917a isolates were significantly observed in Zhanjiang and Dalian. Their genomic analysis identified a 19.5-kb genomic island that disrupted the original *recA* gene. This genomic island had a G + C content of 40%, which was lower than the average 45.4% G + C content in the *V. parahaemolyticus* genome. Eleven ORFs were identified in this genomic island with a second non-*V. parehaemolyticus recA* gene, which has 87%/82% coverage/identity relative to the indigenous *V. parahaemolyticus recA* gene.

To confirm whether this phenomenon is common in other *V. parahaemolyticus* isolates, we conducted a genomic analysis of 1274 public *V. parahaemolyticus* genomes and found that the *recA* gene was disrupted by different genomic islands in 84 genomes. Gene content analysis of these genomic islands divided them into 10 types (Figure 5), of which 70 genomes belonged to Type I (Table S2). This genomic island contains genes encoding glycosaminoglycan attachment site and other functional genes, which might enhance acid resistance (Chen et al., 2020). The original *recA3* allele was disrupted and was assigned as *recA*107 (Figure S2). The isolates with this type of genomic island are increasingly reported in the clinical setting (Chen et al., 2020). Type II genomic island has similar genetic composition relative to Type I, of which original *recA308* allele was disrupted. The second *recA* in Type III genomic island has 87.94% DNA similar to that in Type I. However, Type III genomic island lacks most of the functional genes presented in Types I and II. The potential role of this genomic island remains unclear. For Types IV to Type IX, each type was only found in only one or two genomes. Similarly, most genes in Types IV and VI genomic islands encode hypothetical proteins. Types I and II restriction-modification systems were found in Types V, VII, VIII, IX, and X genomic islands. The genomic island found in ST917a isolates was assigned into Type X.

DISCUSSION

Due to exceptional adaptation to marine environments, *V. parahaemolyticus* is one of the most significant bacterial pathogens for shrimp, fish and molluscs (Baker-Austin et al., 2018). This work aimed to identify the dynamics of *V. parahaemolyticus* in two distinct shrimp aquacultural models by employing MLST to identify their genotypes (Li et al., 2019). By using this method, Hossain et al., (2014) also found that *Aeromonas hydrophila* strains obtained from catfish in the United States were clustered with the ones identified in China and suggested that US catfish isolates emerged from *A. hydrophila* strains of Asian origin. Our results suggest that *V. parahaemolyticus* populations in RAS were more stable over time than *V. parahaemolyticus* populations under TF, which is consistent with the hypothesis proposed by Vadstein et al., (2018). A recent study also analysed the 16S rDNA amplicons by Denaturing Gradient Gel Electrophoresis (PCR/DGGE) to compare the composition of the bacterial communities of rearing water in one TF and one RAS with Atlantic cod larvae (Attramadal et al., 2014). Ordination based on

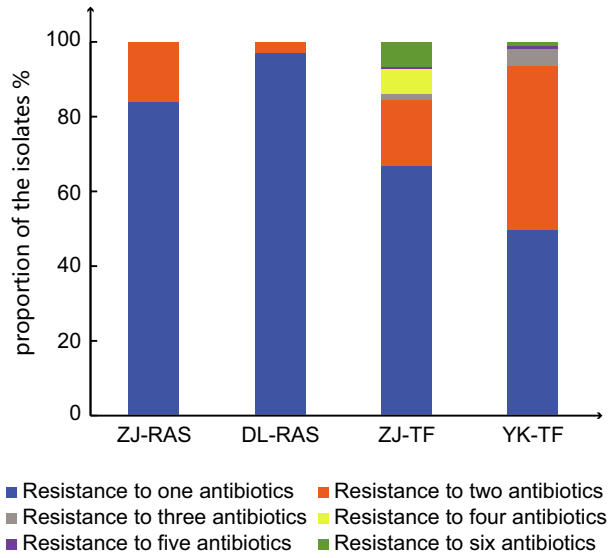

FIGURE 4 Profiles of susceptibility of isolates to 12 antibiotics. The proportion of the isolates that resistant to one or more antibiotic resistance genes are indicated in different colours. ZJ-TF and ZJ-RAS indicates the strains collected from traditional farm and RAS farm in Zhanjiang; YK-TF and DL-RAS indicates the strains collected from traditional farm in Yingkou and RAS farm in Dalian, respectively. Blue: resistance to one antibiotic; orange: resistance to two antibiotics; grey: resistance to three antibiotics; yellow: resistance to four antibiotics; purple: resistance to five antibiotics; green: resistance to six antibiotics. RAS, recirculating aquaculture systems

Bray–Curtis similarity showed there is no significant separation amongst the samples from RAS; however, a clear separation was found within TF samples in terms of the microbial community composition. In addition, the Bray–Curtis similarity was 75% in RAS and 20–25% in TF, indicating the bacterial communities were more stable in RAS. These observations support the microbial management hypothesis concerning the effects of stable water supply on microbial community characteristics.

One limitation of this study was that two farms in the Liaodong Peninsula were within 50 km. Thus, distinct dynamics of the population structure of *V. parahaemolyticus* may have resulted from geographical variability rather than agricultural methods. However, based on our pathogen surveillance on the shrimp farms along the coastal line in this region, many STs were shared amongst different locations and were genetically related within the same STs (Fu et al., 2021b). For instance, ST864, ST1073, ST1166, ST12, ST114 and ST1986 were commonly found in Tangshan, Cangzhou, Dalian and Yingkou located within the Bohai Sea (Figure S1). Likewise, Jiang *et al*. (2019) conducted MLST with *V. parahaemolyticus* and found multiple STs in various locations within the Bohai Sea, suggesting that Dalian and Yingkou might share a similar gene pool. Thus, distinct population dynamics in the two farms might have resulted from specific water exchange ratios. To a large extent, limited water exchange prevented the introduction of pathogens in the RAS

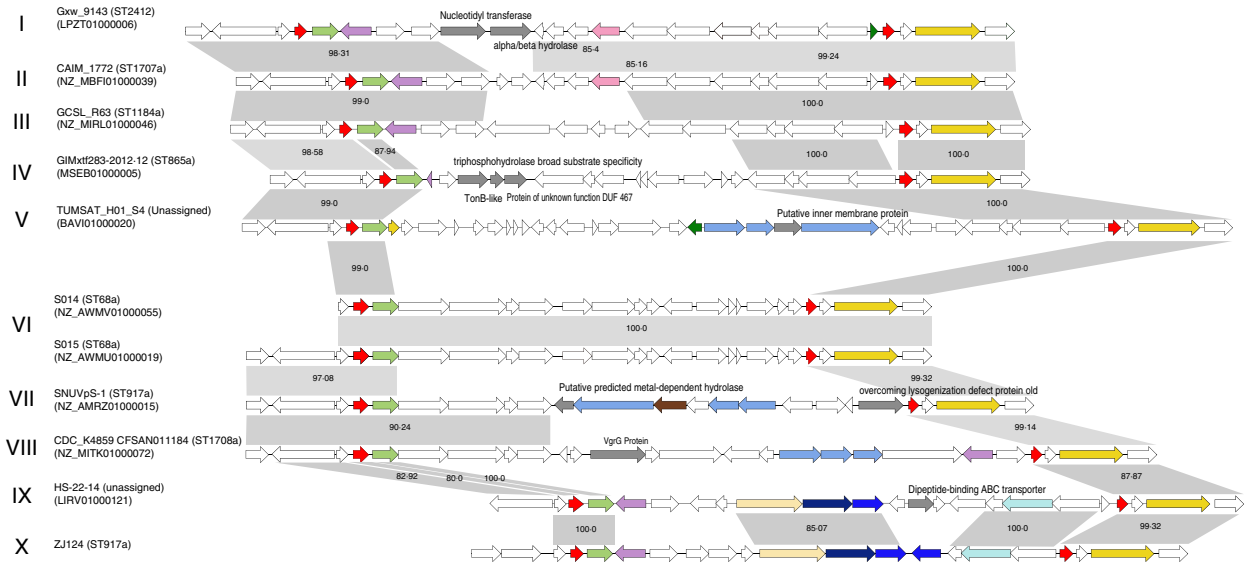

FIGURE 5 Schematic representation of ten types of genomic islands (GIs) inserted into the *recA* site in the *V. parahaemolyticus* strains. The function of genes in GIs is indicated in different colours. The DNA similarity between two regions of the GIs is indicated in grey regions. The distinct functions of genes were represented by different colours: white, hypothetical protein; red, first RecA; light green, second RecA; purple, ParB; dark green, phage integrase; yellow, RecX; light yellow, Type II restriction enzyme YeeA; dark blue, DNA helicase YeeB; bright blue, YeeC-like protein; blue, Type I restriction-modification system; brown, phage protein; sky blue, site-specific recombinase; pink, glycosaminoglycan attachment site

farm, whilst new populations were constantly introduced into the TF farm. Future genomic comparison of *V. parahaemolyticus* in additional RAS and TF farms is needed to support this hypothesis.

Additionally, we found the widespread presence of genomic islands that disrupted the *recA* gene. Coincidentally, recent research reported that *recA* was either unable to be amplified or obtained a PCR product of approximately 1400 bp, almost double that expected size for *recA* (729 bp). González-Escalona *et al*. (2015) further investigated the genetic structure of PCR products in a clinical strain from Peru (090–96) composed of two *recA* fragments from various *Vibrio* spp. Theethakaew et al., (2013) also identified two highly divergent *recA* alleles, *recA*107 and *recA*120, in ST265 and ST251 strains, respectively. Intragenic recombination affecting *recA* has also been reported in *V. cholerae* and *V. mimicus* (Byun et al., 1999; Thompson et al., 2008), suggesting that *recA* may represent a hotspot recombination in *Vibrio* spp. To confirm that the insertion of a genomic island in the *recA* site was universally present in *V. parahaemolyticus* genomes, we conducted a comprehensive investigation from 1274 publicly available genomes. Eighty-four genomes (6.6%) harboured these genomic islands. BLASTN analysis further revealed that the second *recA* sequence introduced by the genomic island was genetically diverse. For instance, the *recA*107 and *recA*120 alleles were matched to the *recA* sequences of *V. cincinnatiensis* (83% similarity) and *V. halioticoli* (83%), respectively, indicating they were possibly acquired by horizontal DNA transfer.

In summary, MLST revealed that the *V. parahaemolyticus* community structure present in the RAS shrimp farm remained stable over time in the 3-year surveillance, which several STs dominated. In contrast, except for three predominant STs (ST114, ST917a and ST1805), the *V. parahaemolyticus* populations were replaced annually in the TF farm. Notably, MDR isolates were frequently identified in TF farms, whilst antibiotic resistance genes were rarely found in the isolates from RAS farms. Pair-wised genomic comparison of isolates from the same STs showed that they were genetically related but belonged to different clones associated with geographical distribution. This study provides significant insights into the population structures of *V. parahaemolyticus* under two distinct aquaculture models, which can help us mitigate the possible emergence of food safety issues.

ACKNOWLEDGEMENTS

We thank for Mr. Xudong Shen for sampling assistance. This research was supported by the National Natural Science Foundation of China (81903372), Youth Fund of Liaoning Provincial Department of Education (QL202005) and Key R&D Program of Guangdong Province (2019B020215001, GML2019ZD0402) and the Special Research Fund of Ghent University (BOF-UGent).

CONFLICT OF INTEREST

The authors declare no competing interests.

AUTHOR CONTRIBUTIONS

Conceived and designed the experiments: Qian Yang and Songzhe Fu. Performed the experiments: Qian Yang, Junmin Wu, Qingyao Wang and Baocheng Qu. Data analysis: Dawei Wei and Yixiang Zhang. Draft and editing of the manuscript: Songzhe Fu, Qian Yang and Ying Liu. All authors approved the final version of the manuscript for submission.

DATA AVAILABILITY STATEMENT

The raw sequencing data were submitted to GenBank (National Center for Biotechnology Information [NCBI]) under BioProject No. PRJNA691968 and PRJNA503785.

ORCID

Songzhe Fu https://orcid.org/0000-0003-1754-199X

REFERENCES

Altschul, S.F., Gish, W., Miller, W., Myers, E.W. & Lipman, D.J. (1990) Basic local alignment search tool. *Journal of Molecular Biology*, 215(3), 403–410.

Attramadal, K.J.K., Truong, T.M.H., Bakke, I., Skjermo, J., Olsen, Y. & Vadstein, O. (2014) RAS and microbial maturation as tools for K-selection of microbial communities improve survival in cod larvae. *Aquaculture*, 432, 483–490.

Aziz, R.K., Bartels, D., Best, A.A., DeJongh, M., Disz, T., Edwards, R.A. et al. (2008) The RAST server: rapid annotation using subsystems technology. *BMC Genomics*, 9, 75.

Baker-Austin, C., Oliver, J.D., Alam, M., Ali, A., Waldor, M.K., Qadri, F. et al. (2018) Vibrio spp. infections. *Nature Reviews Disease Primerss*, 4(1):8.

Bankevich, A., Nurk, S., Antipov, D., Gurevich, A.A., Dvorkin, M., Kulikov, A.S. et al. (2012) SPAdes: a new genome assembly algorithm and its applications to single-cell sequencing. *Journal in Computational Biology*, l19, 455–477.

Birkett, C., Lipscomb, R., Moreland, T., Leeds, T. & Evenhuis, J.P. (2020) Recirculation versus flow-through rainbow trout laboratory *Flavobacterium columnare* challenge. *Diseases of Aquatic Organisms*, 139, 213–221.

Bolger, A.M., Lohse, M. & Usadel, B. (2014) Trimmomatic: A flexible trimmer for Illumina sequence data. *Bioinformatics*, 30, 2114–2120.

Burbridge, P.R. & Hellin, D.C. (2000) Rehabilitation of coastal wetland forests degraded through their conversion to shrimp farms. In: Proceedings of a Conference on Sustainability of Wetlands and Water Resources

Byun, R., Elbourne, L.D., Lan, R. & Reeves, P.R. (1999) Evolutionary relationships of pathogenic clones of *Vibrio cholerae* by sequence analysis of four housekeeping genes. *Infection and Immunity*, 67, 1116–1124.

Carver, T., Harris, S.R., Berriman, M., Parkhill, J. & McQuillan, J.A. (2012) Artemis: an integrated platform for visualization and analysis of high-throughput sequence-based experimental data. *Bioinformatics*, 28, 464–469.

Chan, C.H.S., Octavia, S., Sintchenko, V. & Lan, R. (2016) SnpFilt: a pipeline for reference-free assembly-based identification of SNPs

in bacterial genomes. *Computational Biology and Chemistry*, 65, 178–184.

Chen, X., Li, Y., Yao, W., Wu, T., Zhu, Q., Zhang, Y. et al. (2020) A new emerging serotype of *Vibrio parahaemolyticus* in China is rapidly becoming the main epidemic strain. *Clinical Microbiology & Infection*, 26(5), 644.e1–644.e7.

CLSI (2006) *Methods for antimicrobial dilution and disk susceptibility testing of infrequently isolated or fastidious bacteria*. Wayne: Clinical and Laboratory Standards Institute.

Didelot, X. & Wilson, D.J. (2015) ClonalFrameML: efficient inference of recombination in whole bacterial genomes. *PLoS Computational Biology*, 11(2), e1004041.

FAO (2013) Fisheries and Aquaculture Report No. 1053. Report of the FAO/MARD technical workshop on early mortality syndrome (EMS) or acute hepatopancratic necrosis syndrome (AHPNS) of cultured shrimp (under TCP/VIE/3304), Hanoi, Viet Nam, June 25-27.

Fu, S., Tian, H., Wei, D., Zhang, X. & Liu, Y. (2017) Delineating the origins of *Vibrio parahaemolyticus* isolated from outbreaks of acute hepatopancreatic necrosis disease in Asia by the use of whole genome sequencing. *Frontiers in Microbiology*, 8, 2354.

Fu, S., Wang, Q., Zhang, Y., Yang, Q., Hao, J. & Liu, Y. (2021b) Dynamics and microevolution of *Vibrio parahaemolyticus* populations in shellfish farms. *mSystems*, 6(1), e01161-20.

Fu, S., Yang, Q., Wang, Q., Pang, B., Lan, R. & Qu, B. (2021a) Continuous genomic surveillance monitored the in vivo evolutionary trajectories of Vibrio parahaemolyticus and identified a new virulent genotype. *mSystems*, 6(1), e01254-20.

González-Escalona, N., Jolley, K.A., Reed, E. & Martinez-Urtaza, J. (2017) Defining a core genome multilocus sequence typing scheme for the global epidemiology of *Vibrio parahaemolyticus*. *Journal of Clinical Microbiology*, 55, 1682–1697.

González-Escalona, N., Martinez-Urtaza, J., Romero, J., Espejo, R.T., Jaykus, L.A. & DePaola, A. (2008) Determination of molecular phylogenetics of *Vibrio parahaemolyticus* strains by multilocus sequence typing. *Journal of Bacteriology*, 190(8), 2831–2840.

González-Escalona, N., Gavilan, R.G., Eric, B. & Martinez-Urtaza, J. (2015) Transoceanic spreading of pathogenic strains of Vibrio parahaemolyticus with distinctive genetic signatures in the recA gene. *PLoS One*, 10(2), e0117485.

Hossain, M.J., Sun, D., McGarey, D.J., Wrenn, S., Alexander, L.M., Martino, M.E. et al. (2014) An Asian origin of virulent *Aeromonas hydrophila* responsible for disease epidemics in United States-farmed catfish. *MBio*, 5(3), e00848–e914.

Jiang, Y., Chu, Y., Xie, G., Li, F., Wang, L., Huang, J. et al. (2019) Antimicrobial resistance, virulence and genetic relationship of Vibrio parahaemolyticus in seafood from coasts of Bohai Sea and Yellow Sea, China. *International Journal of Food Microbiology*, 290, 116–124.

Lei, T., Zhang, J., Jiang, F., He, M., Zeng, H., Chen, M. et al. (2019) First detection of the plasmid-mediated colistin resistance gene mcr-1 in virulent *Vibrio parahaemolyticus*. *International Journal of Food Microbiology*, 308, 108290.

Li, Y., Yin, H.Q., Xia, J., Luo, H. & Wang, M.Y. (2019) Population structure and genetic diversity of *Vibrio parahaemolyticus* from a coastal area of China based on a multi-locus sequence typing (MLST) scheme. *Antonie van Leeuwenhoek*, 112(8), 1199–1211.

Niu, B., Hong, B., Zhang, Z., Mu, L., Malakar, P.K., Liu, H. et al. (2018) A novel qPCR method for simultaneous detection and quantification of viable pathogenic and non-pathogenic *Vibrio parahaemolyticus* (*tlh*(+), *tdh*(+), and *ureR* (+)). *Frontiers in Microbiology*, 9, 1747.

Oksanen, J., Blanchet, F.G., Friendly, M., Kindt, R., Legendre, P. & McGlinn, D. et al. (2019) vegan: community ecology package. Available from: https://CRAN.R-project.org/package=vegan. Accessed on July-4, 2020.

R Development Core Team (2014) *R: a language and environment for statistical computing*. Vienna: R Foundation for Statistical Computing.

Stamatakis, A. (2006) RAxML-VI-HPC: maximum likelihood-based phylogenetic analyses with thousands of taxa and mixed models. *Bioinformatics*, 22(21), 2688–2690.

Theethakaew, C., Feil, E.J., Castillo-Ramírez, S., Aanensen, D.M., Suthienkul, O., Neil, D.M. & et al. (2013) Genetic relationships of *Vibrio parahaemolyticus* isolates from clinical, human carrier, and environmental sources in Thailand, determined by multilocus sequence analysis. *Applied and Environment Microbiology*, 79(7), 2358–2370.

Thompson, C.C., Thompson, F.L. & Vicente, A.C.P. (2008) Identification of *Vibrio cholerae* and *Vibrio mimicus* by multilocus sequence analysis (MLSA). *International Journal of Systematic and Evolutionary Microbiology*, 58, 617–621.

Vadstein, O., Attramadal, K.J.K., Bakke, I., Forberg, T., Olsen, Y., Verdegem, M. et al. (2018) Managing the microbial community of marine fish larvae: a holistic perspective for larviculture. *Frontiers in Microbiology*, 27(9), 1820.

Xie, B. & Yu, K. (2007) Shrimp farming in China: operating characteristics, environmental impact and perspectives. *Ocean & Coastal Management*, 50(7), 538–550.

Xie, T., Yu, Q., Tang, X., Zhao, J. & He, X. (2020) Prevalence, antibiotic susceptibility and characterization of *Vibrio parahaemolyticus* isolates in China. *FEMS Microbiology Letters*, 367(16), fnaa136.

Yang, C., Pei, X., Wu, Y., Yan, L., Han, H., Song, Y. et al. (2019) Recent mixing of *Vibrio parahaemolyticus* populations. *The ISME Journal*, 13(10), 2578–2588.

Zankari, E., Hasman, H., Cosentino, S., Vestergaard, M., Rasmussen, S., Lund, O. et al. (2012) Identification of acquired antimicrobial resistance genes. *Journal of Antimicrobial Chemotherapy*, 67(11), 2640–2644.

Zorrilla, I., Chabrillón, M., Arijo, S., Díaz-Rosales, P., Martínez-Manzanares, E., Balebona, M.C. et al. (2003) Bacteria recovered from diseased cultured gilthead sea bream (*Sparus aurata* L.) in southwestern Spain. *Aquaculture*, 218(1–4), 11–20.

SUPPORTING INFORMATION

Additional supporting information may be found online in the Supporting Information section.

How to cite this article: Yang, Q., Wang, Q., Wu, J., Zhang, Y., Wei, D., Qu, B., et al. (2022) Distinct dynamics of *Vibrio parahaemolyticus* populations in two farming models. *Journal of Applied Microbiology*, 133, 1146–1155. https://doi.org/10.1111/jam.15217